

Metric tensors for the interpolation error and its gradient in L^p norm

Hehu Xie* Xiaobo Yin†

Abstract. A uniform strategy to derive metric tensors in two spatial dimension for interpolation errors and their gradients in L^p norm is presented. It generates anisotropic adaptive meshes as quasi-uniform ones in corresponding metric space, with the metric tensor being computed based on a posteriori error estimates in different norms. Numerical results show that the corresponding convergence rates are always optimal.

Keywords. metric tensor, interpolation; gradient; anisotropic.

AMS subject classification. 65N30, 65N50

1 Introduction

Generation of adaptive meshes is now the standard option in most software packages. Traditionally, isotropic mesh adaptation has received much attention, where regular mesh elements are only adjusted in size based on an error estimate. However, for problems with anisotropic solutions (with, say, sharp boundary or internal layers), the shape of elements can be further optimized and an equidistribution of a scalar error density is not sufficient to ensure that a mesh is optimally efficient [14]. Indeed anisotropic meshes have been used successfully in many areas, for example in singular perturbation and flow problems [4–6, 21, 22, 35, 43] and in adaptive procedures [2, 7, 8, 10, 11, 23, 35, 36]. For anisotropic mesh adaptation, the common practice is to generate the needed anisotropic mesh as a quasi-uniform one in the metric space determined by a tensor (or a matrix-valued function), always called monitor function or metric tensor. Both the monitor function (denoted by the letter M) and metric tensor (denoted by the calligraphy letter \mathcal{M}) play the same role in mesh generation, i.e., they are used to specify the size, shape, and orientation of mesh elements throughout the physical domain. The only difference lies in the way they specify the size of elements. Indeed, the former specifies the element size through the

*LSEC, ICMSEC, Academy of Mathematics and Systems Science, CAS, Beijing 100080, China email: hhxie@lsec.cc.ac.cn

†Department of Mathematics, Central China Normal University, Wuhan 430079, China email: yinxb@lsec.cc.ac.cn

equidistribution condition, while the latter determines the element size through the unitary volume requirement. Readers could regard the metric tensor as normalization for the monitor function. Examples of anisotropic meshing strategies include blue refinement [29, 30], directional refinement [36], Delaunay-type triangulation method [7, 8, 11, 35], advancing front method [19], bubble packing method [41], local refinement and modification [21, 37], variational methods [9, 17, 24, 27, 28, 31], and so on. Readers are referred to [18] and [34] for an overview.

Among these meshing strategies, the definition of the metric tensor (or monitor function) based on the Hessian of the solution seems widespread in the meshing community [1, 11–15, 20, 21, 23–26, 37, 39]. Especially, Huang and Russell [26] propose the monitor function

$$M = \det \left(I + \frac{1}{\alpha} |H(u)| \right)^{-\frac{1}{d+p(2-m)}} \left\| I + \frac{1}{\alpha} |H(u)| \right\|^{\frac{mp}{d+p(2-m)}} \left[I + \frac{1}{\alpha} |H(u)| \right], \quad (1.1)$$

for the interpolation error in $W^{m,p}$ norm ($m = 0, 1, p \in [1, +\infty)$), where d stands for the spatial dimension. Set $\mathcal{H} = I + \frac{1}{\alpha} |H(u)|$, when $d = 2$,

$$M_{m,p} = \det(\mathcal{H})^{-\frac{1}{2+p(2-m)}} \|\mathcal{H}\|^{\frac{mp}{2+p(2-m)}} \mathcal{H}. \quad (1.2)$$

Separately, it becomes

$$M_{0,p} = \det(\mathcal{H})^{-\frac{1}{2(p+1)}} \mathcal{H}, \quad (1.3)$$

for the interpolation error in L^p norm and

$$M_{1,p} = \det(\mathcal{H})^{-\frac{1}{p+2}} \|\mathcal{H}\|^{\frac{p}{p+2}} \mathcal{H}. \quad (1.4)$$

for the gradient of interpolation error in L^p norm.

The objective of this paper is to give a unified strategy deriving metric tensors in two spatial dimension for interpolation error and its gradients in L^p norm. The development begin with the error estimates [32] for L^2 norm and our recent work [42] for H^1 norm on linear interpolation for quadratic functions on triangles. These estimates are anisotropic in the sense that they allow a full control of the shape of elements when used within a mesh generation strategy. Using the relationship between different norms, a posterior error estimates for other norms ($W^{m,p}, m = 0, 1, p \neq 2$) can be gained. We will apply these error estimates to formulate corresponding metric tensors in a unified way. The procedure is based on two considerations: on the one hand the anisotropic mesh is generated as a quasi-uniform mesh in the metric tensor. On the other hand, the anisotropic mesh is required to minimize the error for a given number of triangles. To compare with those existing methods, we list our main results using monitor function style, that is

$$M_{0,p}^n(\mathbf{x}) = \det(\mathcal{H})^{-\frac{1}{2(p+1)}} \mathcal{H}, \quad (1.5)$$

for interpolation errors in L^p norm and

$$M_{1,p}^n(\mathbf{x}) = \det(\mathcal{H})^{-\frac{1}{p+2}} \text{tr}(\mathcal{H})^{\frac{p}{p+2}} \mathcal{H}, \quad (1.6)$$

for gradient of interpolation errors in L^p norm. To sum up, the metric tensor can be expressed by

$$M_{m,p}^n(\mathbf{x}) = \det(\mathcal{H})^{-\frac{1}{2+p(2-m)}} \operatorname{tr}(\mathcal{H})^{\frac{mp}{2+p(2-m)}} \mathcal{H}, \quad (1.7)$$

for the $W^{m,p}$ norm ($m = 0, 1, p \in (0, +\infty]$) of the interpolation error.

The paper is organized as follows. In Section 2, we describe the anisotropic error estimates on linear interpolation for quadratic functions on triangles obtained in our recent work [42]. The formulation of the monitor function and metric tensor is developed in Section 3. Numerical results are presented in Section 4 to illustrating our analysis. Finally, conclusions are drawn in Section 5.

2 Estimates for interpolation error and its gradient

As we know, the interpolation error depends on the solution, the size and shape of the elements in the mesh. Understanding this relation is crucial for the generating efficient meshes for the finite element method. In the mesh generation community, this relation is studied more closely for the model problem of interpolating quadratic functions. This treatment yields a reliable and efficient estimator of the interpolation error for general functions provided a saturation assumption is valid [3, 16]. For instance, Nadler [32] derived an exact expression for the L^2 -norm of the linear interpolation error in terms of the three sides ℓ_1, ℓ_2 , and ℓ_3 of the triangle K ,

$$\|u - u_I\|_{L^2(K)}^2 = \frac{|K|}{180} \left[(d_1 + d_2 + d_3)^2 + d_1 d_2 + d_2 d_3 + d_1 d_3 \right], \quad (2.1)$$

where $|K|$ is the area of the triangle, $d_i = \ell_i \cdot H \ell_i$ with H being the Hessian of u . Assuming $u = \lambda_1 x^2 + \lambda_2 y^2$, D'Azevedo and Simpson [13] derived the exact formula for the maximum norm of the interpolation error

$$\|(u - u_I)\|_{L^\infty(K)}^2 = \frac{D_{12} D_{23} D_{31}}{16 \lambda_1 \lambda_2 |K|^2}, \quad (2.2)$$

where $D_{ij} = \ell_i \cdot \operatorname{diag}(\lambda_1, \lambda_2) \ell_j$. Based on the geometric interpretation of this formula, they proved that for a fixed area the optimal triangle, which produces the smallest maximum interpolation error, is the one obtained by compressing an equilateral triangle by factors $\sqrt{\lambda_1}$ and $\sqrt{\lambda_2}$ along the two eigenvectors of the Hessian of u . Furthermore, the optimal incidence for a given set of interpolation points is the Delaunay triangulation based on the stretching map (by factors $\sqrt{\lambda_1}$ and $\sqrt{\lambda_2}$ along the two eigenvector directions) of the grid points. Rippa [38] showed that the mesh obtained in this way is also optimal for the L^p -norm of the error for any $1 \leq p \leq \infty$.

The element-wise error estimates in the following theorem are developed in [42] using the theory of interpolation and proper numerical quadrature formula.

Theorem 2.1. *Let u be a quadratic function and u_I is the Lagrangian linear finite element interpolation of u . The following relationship holds:*

$$\|\nabla(u - u_I)\|_{L^2(K)}^2 = \frac{1}{48|K|} \sum_{i=1}^3 (\ell_{i+1} \cdot H\ell_{i+2})^2 |\ell_i|^2, \quad (2.3)$$

where we prescribe $i + 3 = i, i - 3 = i$.

To get the a posteriori error estimate of the interpolation error in L^p and $W^{1,p}$ norms for $p \neq 2$, we need some lemmas below.

Lemma 2.1. *For any d positive numbers a_1, \dots, a_d , the inequalities*

$$\left(\sum_{j=1}^d a_j^2\right)^{\frac{1}{2}} \leq \left(\sum_{j=1}^d a_j^p\right)^{\frac{1}{p}} \leq d^{\frac{1}{p}-\frac{1}{2}} \left(\sum_{j=1}^d a_j^2\right)^{\frac{1}{2}}, \quad (2.4)$$

and

$$d^{\frac{1}{p}-\frac{1}{2}} \left(\sum_{j=1}^d a_j^2\right)^{\frac{1}{2}} \leq \left(\sum_{j=1}^d a_j^p\right)^{\frac{1}{p}} \leq \left(\sum_{j=1}^d a_j^2\right)^{\frac{1}{2}} \quad (2.5)$$

hold for numbers $0 < p < 2$ and $p > 2$, respectively.

Proof. We just give the proof for the case $0 < p < 2$, it is similar for the case $p > 2$.

For any number $0 < p < 2$,

$$\left(\sum_{j=1}^d a_j^2\right)^{\frac{1}{2}} \leq \left(\sum_{j=1}^d a_j^p\right)^{\frac{1}{p}}$$

holds due to the Jensen's inequality. From the generalized arithmetic-mean geometric-mean inequality, for any positive numbers a_1, \dots, a_d ,

$$\left(\sum_{j=1}^d \frac{1}{d} a_j^p\right)^{\frac{1}{p}} \leq \left(\sum_{j=1}^d \frac{1}{d} a_j^2\right)^{\frac{1}{2}}.$$

Then

$$\left(\sum_{j=1}^d a_j^p\right)^{\frac{1}{p}} \leq d^{\frac{1}{p}-\frac{1}{2}} \left(\sum_{j=1}^d a_j^2\right)^{\frac{1}{2}}.$$

□

To sum up, for any d positive numbers a_1, \dots, a_d , the inequalities

$$\underline{C}_p \left(\sum_{j=1}^d a_j^2\right)^{\frac{1}{2}} \leq \left(\sum_{j=1}^d a_j^p\right)^{\frac{1}{p}} \leq \overline{C}_p \left(\sum_{j=1}^d a_j^2\right)^{\frac{1}{2}} \quad (2.6)$$

holds for any numbers $p > 0$, where $\underline{C}_p = 1$ for $0 < p < 2$ and $d^{\frac{1}{p}-\frac{1}{2}}$ for $p > 2$, $\overline{C}_p = d^{\frac{1}{p}-\frac{1}{2}}$ for $0 < p < 2$ and 1 for $p > 2$.

Lemma 2.2. [3] For any $p \in (0, +\infty]$ and any non-negative $v \in P_2(K)$ it holds

$$C_{1/p}^{-\frac{1}{p}} |K|^{\frac{1}{p}-1} \|v\|_{L^1(K)} \leq \|v\|_{L^p(K)} \leq C_p |K|^{\frac{1}{p}-1} \|v\|_{L^1(K)} \quad (2.7)$$

with

$$\begin{cases} C_p = 1 & \text{if } 0 < p \leq 1, \\ C_p = (d+1)(d+2)(d!)^{\frac{1}{p}} \left(\prod_{j=1}^d (p+j) \right)^{-\frac{1}{p}} & \text{if } 1 < p < +\infty, \\ C_\infty = \lim_{p \rightarrow +\infty} C_p = (d+1)(d+2), \\ C_{1/\infty} = \lim_{p \rightarrow +\infty} C_{1/p} = 1. \end{cases}$$

2.1 Estimates for interpolation errors in L^p norm

We consider the error of linear interpolation $e = u - u_I$ for a quadratic function u on K . Since the function e is quadratic on K , we can apply Lemma 2.2 to obtain

$$C_{1/p}^{-1/p} |K|^{\frac{1}{p}-1} \|e\|_{L^1(K)} \leq \|e\|_{L^p(K)} \leq C_p |K|^{\frac{1}{p}-1} \|e\|_{L^1(K)}. \quad (2.8)$$

Set $p = 2$,

$$|K|^{-\frac{1}{2}} \|e\|_{L^1(K)} \leq \|e\|_{L^2(K)} \leq C_2 |K|^{-\frac{1}{2}} \|e\|_{L^1(K)},$$

or

$$C_2^{-1} |K|^{\frac{1}{2}} \|e\|_{L^2(K)} \leq \|e\|_{L^1(K)} \leq |K|^{\frac{1}{2}} \|e\|_{L^2(K)}. \quad (2.9)$$

Combine (2.8) and (2.9), we get

$$C_{1/p}^{-1/p} C_2^{-1} |K|^{\frac{1}{p}-\frac{1}{2}} \|e\|_{L^2(K)} \leq \|e\|_{L^p(K)} \leq C_p |K|^{\frac{1}{p}-\frac{1}{2}} \|e\|_{L^2(K)}. \quad (2.10)$$

In this article, $A \sim B$ stands for that there exist two constants \underline{C} and \overline{C} such that

$$\underline{C}A \leq B \leq \overline{C}A,$$

where the two constants \underline{C} and \overline{C} may depend on the prescribed error, the index p , the dimension d , and the numbers of elements N , however are independent of function at hand. So (2.10) can be rewritten as

$$\|e\|_{L^p(K)} \sim |K|^{\frac{1}{p}-\frac{1}{2}} \|e\|_{L^2(K)}.$$

Together with the expression (2.1) for the L^2 norm of the linear interpolation error derived by Nadler [32], we have the a posteriori error estimate in L^p norms as follows:

$$\|e\|_{L^p(K)}^2 \sim |K|^{\frac{2}{p}-1} \|e\|_{L^2(K)}^2 = \frac{|K|^{\frac{2}{p}}}{180} \left[\left(\sum_{i=1}^3 d_i \right)^2 + d_1 d_2 + d_2 d_3 + d_1 d_3 \right]. \quad (2.11)$$

2.2 Estimates for gradient of interpolation errors in L^p norm

Now we consider the gradient of linear interpolation error $\nabla e = \nabla(u - u_I)$ for a quadratic function u . Since the function

$$v_j(x) = \left(\frac{\partial e}{\partial x_j} \right)^2$$

is quadratic on K , we can apply Lemma 2.2 to obtain

$$\|v_j\|_{L^{p/2}(K)}^{1/2} \geq C_{2/p}^{-1/p} |K|^{\frac{1}{p}-\frac{1}{2}} \|v_j\|_{L^1(K)}^{1/2} = C_{2/p}^{-1/p} |K|^{\frac{1}{p}-\frac{1}{2}} \left\| \frac{\partial e}{\partial x_j} \right\|_{L^2(K)}, \quad (2.12)$$

and

$$\|v_j\|_{L^{p/2}(K)}^{1/2} \leq C_{p/2}^{1/2} |K|^{\frac{1}{p}-\frac{1}{2}} \|v_j\|_{L^1(K)}^{1/2} = C_{p/2}^{1/2} |K|^{\frac{1}{p}-\frac{1}{2}} \left\| \frac{\partial e}{\partial x_j} \right\|_{L^2(K)}. \quad (2.13)$$

Since

$$\|\nabla e\|_{L^p(K)}^p = \sum_{j=1}^d \int_K \left| \frac{\partial e}{\partial x_j} \right|^p d\mathbf{x} = \sum_{j=1}^d \|v_j\|_{L^{p/2}(K)}^{p/2},$$

then together with (2.12) and (2.13), we have

$$C_{2/p}^{-1/p} |K|^{\frac{1}{p}-\frac{1}{2}} \left(\sum_{j=1}^d \left\| \frac{\partial e}{\partial x_j} \right\|_{L^2(K)}^p \right)^{\frac{1}{p}} \leq \|\nabla e\|_{L^p(K)} \leq C_{p/2}^{1/2} |K|^{\frac{1}{p}-\frac{1}{2}} \left(\sum_{j=1}^d \left\| \frac{\partial e}{\partial x_j} \right\|_{L^2(K)}^p \right)^{\frac{1}{p}}.$$

From (2.6), the inequality

$$\underline{C}_p C_{2/p}^{-1/p} |K|^{\frac{1}{p}-\frac{1}{2}} \|\nabla e\|_{L^2(K)} \leq \|\nabla e\|_{L^p(K)} \leq \overline{C}_p C_{p/2}^{1/2} |K|^{\frac{1}{p}-\frac{1}{2}} \|\nabla e\|_{L^2(K)},$$

holds, or simply

$$\|\nabla e\|_{L^p(K)} \sim |K|^{\frac{1}{p}-\frac{1}{2}} \|\nabla e\|_{L^2(K)}.$$

Together with the a posteriori error estimate (2.3) of the interpolation error in $H^1(= W^{1,2})$ norm, we have the a posteriori error estimate in $W^{1,p}$ norms as follows:

$$\begin{aligned} \|\nabla e\|_{L^p(K)}^2 &\sim |K|^{\frac{2}{p}-1} \|\nabla e\|_{L^2(K)}^2 \\ &= |K|^{\frac{2}{p}-1} \frac{1}{48|K|} \sum_{i=1}^3 (\ell_{i+1} \cdot H_K \ell_{i+2})^2 |\ell_i|^2 \\ &= \frac{|K|^{\frac{2}{p}-2}}{48} \sum_{i=1}^3 (\ell_{i+1} \cdot H_K \ell_{i+2})^2 |\ell_i|^2. \end{aligned} \quad (2.14)$$

3 Metric tensors for anisotropic mesh adaptation

We now use the results of Section 2 to develop metric tensors for interpolation errors and their gradients in L^p norm in a unified way. As a common practice in anisotropic mesh generation, the metric tensor, $\mathcal{M}(\mathbf{x})$, is used in a meshing strategy in such a way that an anisotropic mesh is generated as a quasi-uniform mesh in the metric space determined by $\mathcal{M}(\mathbf{x})$. Mathematically, this can be interpreted as the shape, size and equidistribution requirements as follows.

The shape requirement. The elements of the new mesh, \mathcal{T}_h , are (or are close to being) equilateral in the metric.

The size requirement. The elements of the new mesh \mathcal{T}_h have a unitary volume in the metric, i.e.,

$$\int_K \sqrt{\det(\mathcal{M}(\mathbf{x}))} dx = 1, \quad \forall K \in \mathcal{T}_h. \quad (3.1)$$

The equidistribution requirement. The anisotropic mesh is required to minimize the error for a given number of mesh points (or equidistribute the error on every element).

Notice that to derive the monitor function, we just need the shape and equidistribution requirements.

3.1 Metric tensors for gradients of interpolation errors in L^p norm

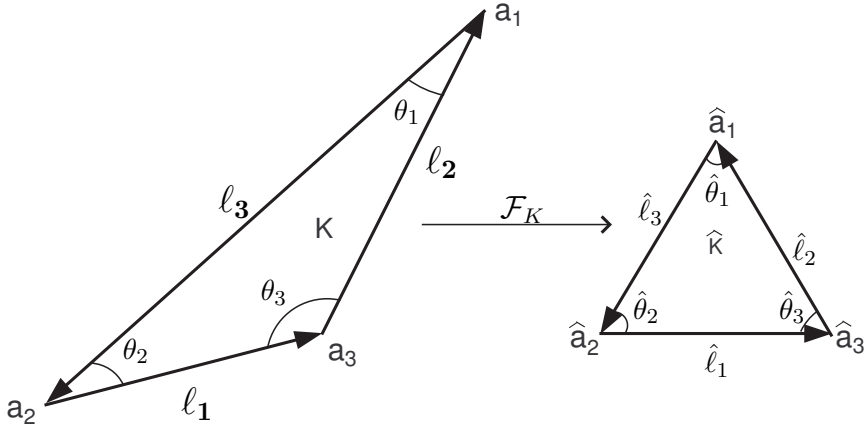


Figure 1: Affine map $\hat{\mathbf{x}} = \mathcal{F}_K \mathbf{x}$ from K to the reference triangle \hat{K} .

We derive the monitor function $M(\mathbf{x})$ first. Assume $H(u)$ be a symmetric positive definite matrix on every point \mathbf{x} , this assumption will be dropped later. Set $M(\mathbf{x}) = C(\mathbf{x})H(u)$. Consider the L^2 projection of $H(u)$ on K , denoted by H_K , then so does M_K . Since H_K is a symmetric positive definite matrix, we consider the singular value decomposition $H_K = R^T \Lambda R$, where $\Lambda = \text{diag}(\lambda_1, \lambda_2)$ is the diagonal matrix of the corresponding eigenvalues

($\lambda_1, \lambda_2 > 0$) and R is the orthogonal matrix having as rows the eigenvectors of H_K . Denote by F_K and \mathbf{t}_K the matrix and the vector defining the invertible affine map $\hat{\mathbf{x}} = \mathcal{F}_K(\mathbf{x}) = F_K \mathbf{x} + \mathbf{t}_K$ from the generic element K to the reference triangle \hat{K} (see Figure 1).

Obviously, $M_K = C_K H_K$. Let $M_K = F_K^T F_K$, then $F_K = C_K^{\frac{1}{2}} \Lambda^{\frac{1}{2}} R$. Mathematically, the shape requirement can be expressed as

$$|\hat{\ell}_i| = L \text{ and } \cos \hat{\theta}_i = \frac{\hat{\ell}_{i+1} \cdot \hat{\ell}_{i+2}}{L^2} = \frac{1}{2}, \quad i = 1, 2, 3, \quad (3.2)$$

where L is a constant for every element K . Enforcing the shape requirement, we get

$$\begin{aligned} \|\nabla e\|_{L^p(K)}^2 &\sim \frac{|K|^{\frac{2}{p}-2}}{48} \sum_{i=1}^3 (\ell_{i+1} \cdot H_K \ell_{i+2})^2 |\ell_i|^2 \\ &= \frac{|K|^{\frac{2}{p}-2}}{48 C_K^2} \sum_{i=1}^3 (\ell_{i+1} \cdot M_K \ell_{i+2})^2 |\ell_i|^2 \\ &= \frac{L^4 |K|^{\frac{2}{p}-2}}{48 C_K^2} \sum_{i=1}^3 (\cos \hat{\theta}_i)^2 |\ell_i|^2 = \frac{L^4 |K|^{\frac{2}{p}-2}}{192 C_K^2} \sum_{i=1}^3 |\ell_i|^2. \end{aligned}$$

Notice that,

$$|K| = \frac{|\hat{K}|}{C_K \sqrt{\det(H_K)}},$$

we have

$$\begin{aligned} \|\nabla e\|_{L^p(K)}^2 &\sim \frac{L^4 |\hat{K}|^{\frac{2}{p}-2} C_K^{2-\frac{2}{p}} \det(H_K)^{1-\frac{1}{p}}}{192 C_K^2} \sum_{i=1}^3 \left| C_K^{-\frac{1}{2}} R^{-1} \Lambda^{-\frac{1}{2}} \hat{\ell}_i \right|^2 \\ &= \frac{L^4 |\hat{K}|^{\frac{2}{p}-2} \det(H_K)^{1-\frac{1}{p}}}{192 C_K^{1+\frac{2}{p}}} \sum_{i=1}^3 \left| \Lambda^{-\frac{1}{2}} \hat{\ell}_i \right|^2 \\ &= \frac{L^4 |\hat{K}|^{\frac{2}{p}-2} \det(H_K)^{1-\frac{1}{p}} \operatorname{tr}(H_K)}{192 C_K^{1+\frac{2}{p}} \det(H_K)} \\ &= \frac{L^4 |\hat{K}|^{\frac{2}{p}-2} \det(H_K)^{-\frac{1}{p}} \operatorname{tr}(H_K)}{192 C_K^{1+\frac{2}{p}}} \\ &\sim \frac{\det(H_K)^{-\frac{1}{p}} \operatorname{tr}(H_K)}{C_K^{1+\frac{2}{p}}}, \end{aligned}$$

then

$$\|\nabla e\|_{L^p(K)}^p = (\|\nabla e\|_{L^p(K)}^2)^{p/2} \sim \frac{\det(H_K)^{-\frac{1}{2}} \operatorname{tr}(H_K)^{\frac{p}{2}}}{C_K^{1+\frac{p}{2}}}.$$

To satisfy the equidistribution requirement, let

$$\|\nabla e\|_{L^p(K)}^p = \left(\sum_{K \in \mathcal{T}_h} e_K^p \right) / N = \epsilon^p / N,$$

where N is the number of elements of \mathcal{T}_h . Then

$$C_K \sim \det(H_K)^{-\frac{1}{p+2}} \text{tr}(H_K)^{\frac{p}{p+2}}.$$

So $M(\mathbf{x})$ could be the form

$$M(\mathbf{x}) = \det(H)^{-\frac{1}{p+2}} \text{tr}(H)^{\frac{p}{p+2}} H(u),$$

since $M(\mathbf{x})$ can be modified by multiplying a constant. Since it corresponds the gradient of interpolation errors in L^p norm, we denote it by $M_{1,p}^n(\mathbf{x})$.

To establish the metric tensor $\mathcal{M}_{1,p}^n(\mathbf{x})$, set $\mathcal{M}_{1,p}^n(\mathbf{x}) = \theta_{1,p} M_{1,p}^n(\mathbf{x})$, at this time, the size requirement (3.1) should be used, which leads to

$$\theta_{1,p} \int_K \rho_{1,p}(\mathbf{x}) d\mathbf{x} = 1,$$

where

$$\rho_{1,p}(\mathbf{x}) = \sqrt{\det(M_{1,p}^n(\mathbf{x}))}.$$

Summing the above equation over all the elements of \mathcal{T}_h , one gets

$$\theta_{1,p} \sigma_{1,p} = N,$$

where

$$\sigma_{1,p} = \int_{\Omega} \rho_{1,p}(\mathbf{x}) d\mathbf{x}.$$

Thus, we get

$$\theta_{1,p} = \frac{N}{\sigma_{1,p}},$$

and as a consequence,

$$\mathcal{M}_{1,p}^n(\mathbf{x}) = \frac{N}{\sigma_{1,p}} \det(H)^{-\frac{1}{p+2}} \text{tr}(H)^{\frac{p}{p+2}} H(u).$$

3.2 Metric tensor for the interpolation errors in L^p norm

Using the error estimates (2.11) for interpolation errors in L^p norm and the shape requirement (3.2), we have

$$\begin{aligned} \|e\|_{L^p(K)}^2 &\sim \frac{|K|^{\frac{2}{p}}}{180} \left[\left(\sum_{i=1}^3 d_i \right)^2 + d_1 d_2 + d_2 d_3 + d_1 d_3 \right] \\ &= \frac{|K|^{\frac{2}{p}}}{180 C_K^2} \left[\left(\sum_{i=1}^3 |\hat{\ell}_i|^2 \right)^2 + \sum_{i=1}^3 \left(|\hat{\ell}_{i+1}| |\hat{\ell}_{i+2}| \right)^2 \right] \\ &= \frac{L^4 |K|^{\frac{2}{p}}}{15 C_K^2} = \frac{L^4 |\hat{K}|^{\frac{2}{p}}}{15 C_K^{2+\frac{2}{p}} \det(H)^{\frac{1}{p}}} \sim \frac{1}{C_K^{2+\frac{2}{p}} \det(H)^{\frac{1}{p}}}. \end{aligned}$$

Then,

$$\|e\|_{L^p(K)}^p = (\|e\|_{L^p(K)}^2)^{p/2} \sim \frac{1}{C_K^{p+1} \det(H)^{\frac{1}{2}}}.$$

To satisfy the equidistribution requirement, let

$$\|e\|_{L^p(K)}^p = \left(\sum_{K \in \mathcal{T}_h} e_K^p \right) / N = \epsilon^p / N.$$

Using similar argument in last subsection, we easily get monitor functions

$$M_{0,p}^n(\mathbf{x}) = \det(H)^{-\frac{1}{2(p+1)}} H(u),$$

and metric tensors

$$\mathcal{M}_{0,p}^n(\mathbf{x}) = \frac{N}{\sigma_{0,p}} \det(H)^{-\frac{1}{2(p+1)}} H(u),$$

for the interpolation errors in L^p norm.

3.3 Practice use of metric tensor

So far we assume that $H(u)$ is a symmetric positive definite matrix at every point. However this assumption doesn't hold in many cases. In order to obtain a symmetric positive definite matrix, the following procedure are often implemented. First, the Hessian H is modified into $|H| = R^T \text{diag}(|\lambda_1|, |\lambda_2|) R$ by taking the absolute value of its eigenvalues ([22]). Since $|H|$ is only semi-positive definite, $\mathcal{M}_{m,p}^n$ cannot be directly applied to generate the anisotropic meshes. To avoid this difficulty, we regularize the expression with the flooring parameter $\alpha_{m,p} > 0$ (see, e.g., [24]). Replacing $|H|$ with

$$\mathcal{H} = \alpha_{m,p} I + |H|,$$

we get the modified metric tensors, also denoted by $\mathcal{M}_{m,p}^n$, that is

$$\mathcal{M}_{m,p}^n(\mathbf{x}) = \frac{N}{\sigma_{m,p}} \det(\mathcal{H})^{-\frac{1}{2+p(2-m)}} \text{tr}(\mathcal{H})^{\frac{mp}{2+p(2-m)}} \mathcal{H}, \quad (3.3)$$

which are suitable for practical mesh generation.

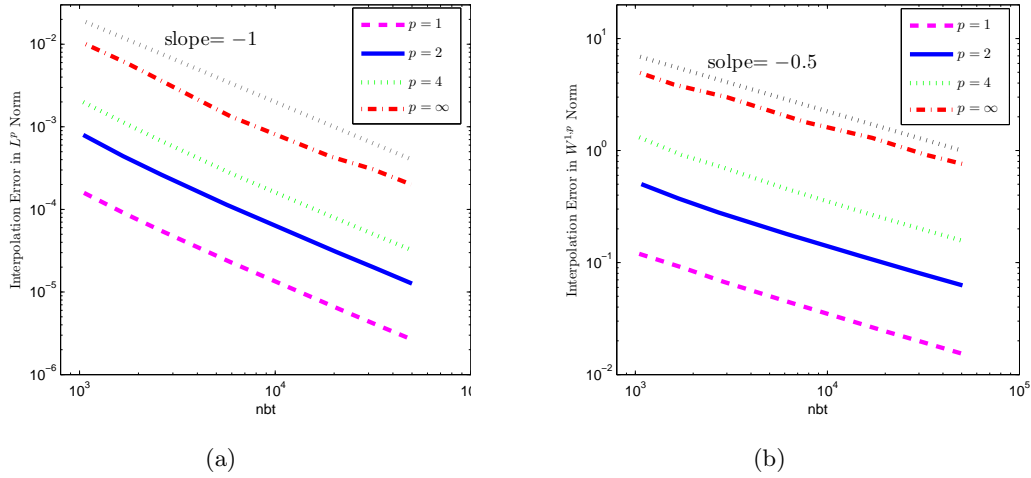


Figure 2: Example 1: Interpolation error and its gradient in L^p norm

3.4 Comparison with existing methods using monitor function style

When $m = 0$, the new monitor function $M_{0,p}^n$ (1.5) is in fact the same with (1.3) in [25, 26]. Chen, Sun and Xu [12] proved that under suitable conditions, the error estimate

$$\|u - u_I\|_{L^p(\Omega)} \leq CN^{-\frac{2}{d}} \|\sqrt[d]{\det H}\|_{L^{\frac{pd}{2p+d}}(\Omega)}, 1 \leq p \leq \infty,$$

holds on the quasi-uniform mesh determined by the metric $(\det H)^{-\frac{1}{2p+d}} H$, where H is a majorant of the Hessian matrix, N is the number of elements in the triangulation and the constant C does not depend on u and N . This estimate is optimal in the sense that it is a lower bound if u is strictly convex or concave. Note that \mathcal{H} can be chosen as a majorant of the Hessian matrix.

When $m = 1$, the new monitor function $M_{1,p}^n$ (1.6) is different with (1.4) [26] that the former refers to $\text{tr}(\mathcal{H})$ and the latter involves $\|\mathcal{H}\|$. In some cases, the two monitor functions are pretty much alike. However, in other cases, the effect of the former is superior to the latter for mesh generation. Numerical results in [40] have shown our approach's superiority for the error in H^1 norm.

4 Numerical experiments

In this section, we present some numerical results for three problems with given analytical solutions. The numerical results are performed by using the BAMG software [23]. Given a background mesh and an approximation solution, BAMG generates the mesh according to the metric tensor. The code allows the user to supply his/her own metric tensor defined on a background mesh. In our computation, the background mesh has been taken as the most recent mesh available.

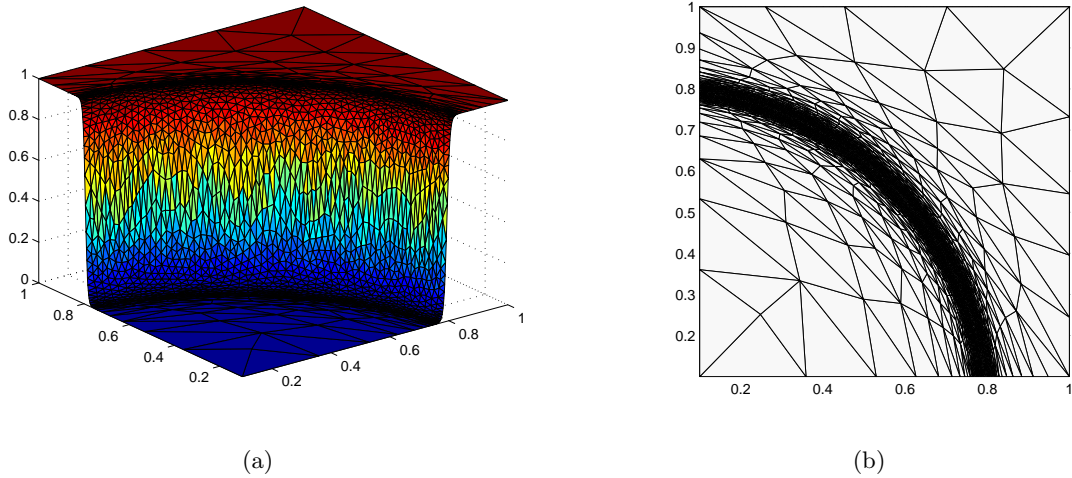


Figure 3: Example 1: plots of the solution (a) and corresponding mesh (b) using $\mathcal{M}_{1,1}$

Denote by nbt the number of triangles in the current mesh. The number of triangles is adjusted when necessary by trial and errors through the modification of the multiplicative coefficient of the metric tensors.

Example 1 This example is to generate adaptive meshes for

$$u(\mathbf{x}) = \frac{1}{1 + e^{-200(\sqrt{x_1^2 + x_2^2} - 0.8)}}, \quad \mathbf{x} \in (0.1, 1) \times (0.1, 1). \quad (4.1)$$

This function is anisotropic along the quarter circle $x_1^2 + x_2^2 = 0.8^2$ and changes sharply in the direction normal to this curve. A similar example was presented in [33] where the region is $(0, 1) \times (0, 1)$. In the current computation, each run is stopped after 15 iterations to guarantee that the adaptive procedure tends towards stability. We show in Figure 2 the L^p norms of the interpolation error and its gradient using corresponding metric tensors, for $p = 1, 2, 4, \infty$. For example, the curve $p = 2$ in (a) stands for the interpolation error using the metric tensor $\mathcal{M}_{0,2}$, while $p = \infty$ in (b) stands for the gradient interpolation error using the metric tensor $\mathcal{M}_{1,\infty}$. We see that the convergence rates for the interpolation error and its gradient are always nearly optimal, i.e. $\|e\|_{L^p} \sim N^{-1}$ and $\|\nabla e\|_{L^p} \sim N^{-0.5}$. We also show in Figure 3 plots of the solution and corresponding mesh using the metric tensor $\mathcal{M}_{1,1}$.

Example 2 This example is to generate adaptive meshes for

$$u(\mathbf{x}) = x_1^2 x_2 + x_2^3 + \tanh(10(\sin(5x_2) - 2x_1)), \quad \mathbf{x} \in (-1, 1) \times (-1, 1). \quad (4.2)$$

This function is anisotropic along the zigzag curve $\sin(5x_2) - 2x_1 = 0$ and changes sharply in the direction normal to this curve (taken from [3]). In the current computation, each run is stopped after 20 iterations to guarantee that the adaptive procedure tends towards stability. We show in Figure 4 the L^p norms of the interpolation error and its gradient

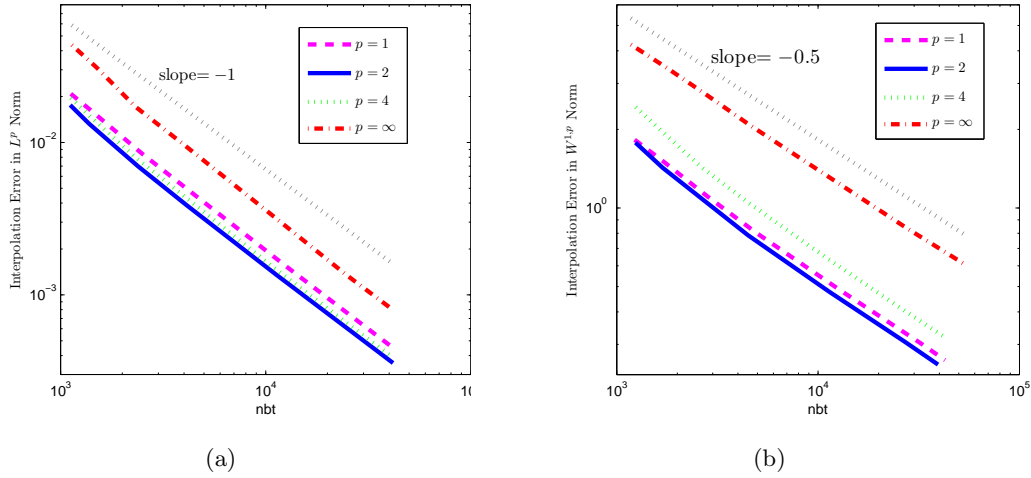


Figure 4: Example 2: Interpolation error and its gradient in L^p norm

using corresponding metric tensors, for $p = 1, 2, 4, \infty$. As in Example 1, the convergence rates for the interpolation error and its gradient here are always nearly optimal. In Figure 5 we select 6 meshes with 4000 triangles generated by corresponding metric tensors. We can learn that the optimal meshes in different norms are different. For example, the mesh generated by the metric tensor $\mathcal{M}_{1,\infty}$ concentrates more triangles and nodes along the zigzag line.

Example 3 (Taken from [40]) This example is to solve the boundary value problem of Poisson's equation

$$-\Delta u = f, \quad \mathbf{x} \in \Omega \equiv (-1.2, 1.2) \times (-1.2, 1.2), \quad (4.3)$$

with the Dirichlet boundary condition and the right-hand side term being chosen such that the exact solution is given by

$$u(\mathbf{x}) = \sum_{i=1}^5 \left[\left(1 + e^{\frac{x+y-c_i}{2\epsilon}}\right)^{-1} + \left(1 + e^{\frac{x-y-d_i}{2\epsilon}}\right)^{-1} \right], \quad (4.4)$$

where $c_i = 0, -0.6, 0.6, -1.2, 1.2$; $d_i = 0, -0.6, 0.6, -1.2, 1.2$. The solution exhibits ten sharp layers on lines $x+y-c_i=0$ and $x-y-d_i=0$, $i = 1, 2, \dots, 5$, when ϵ is small. In our computations, ϵ is taken as 0.01. Numerical results in [40] have shown that our approach's superiority for the error in H^1 norm. In the current computation, each run is stopped after 20 iterations to guarantee that the adaptive procedure tends towards stability, except that governed by $\mathcal{M}_{1,\infty}$, which need 30 iterations. We show in Figure 6 the L^p norms of the interpolation error and its gradient using corresponding metric tensors, for $p = 1, 2, 4, \infty$. As in Example 1 and Example 2, the convergence rates for the interpolation error and its gradient here are always nearly optimal. Another purpose to select this example is to describe the difference of finding layers using different norms. In Figure 7 we list meshes in

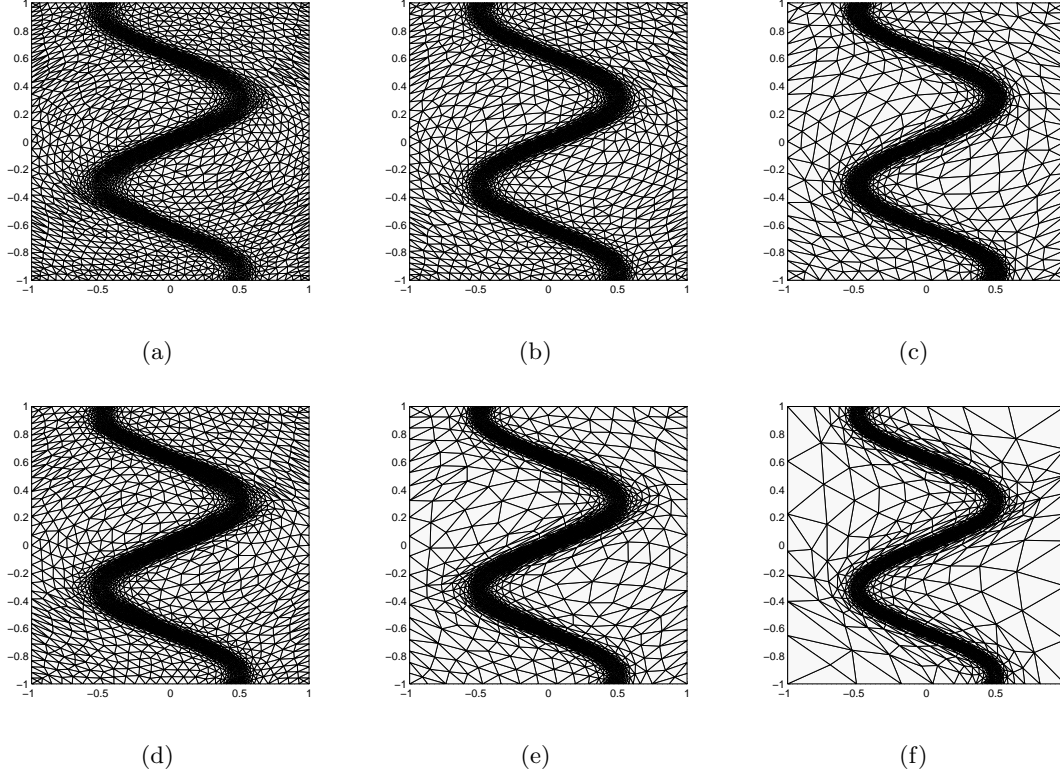


Figure 5: Example 2: Meshes generated by the metric tensor $\mathcal{M}_{m,p}$ for (a) $m = 0, p = 1$, (b) $m = 0, p = 2$, (c) $m = 0, p = \infty$, (d) $m = 1, p = 1$, (e) $m = 1, p = 2$, (f) $m = 1, p = \infty$.

different stage during one selected run governed by corresponding metric tensors. While in Figure 8 convergence history is shown. From the three figures we can learn that most of the metric tensors can quickly find the layers except the metric tensor $\mathcal{M}_{1,\infty}$ when dealing with the complex problems, e.g., with multiple layers.

5 Conclusions

In the previous sections we have developed a uniform strategy to derive metric tensors in two spatial dimension for interpolation errors and their gradients in L^p norm. The metric tensor $\mathcal{M}_{0,p}^n$ for the L^p norm of the interpolation error is similar to some existing methods. However, the metric tensor $\mathcal{M}_{1,p}^n$ is essentially different with those metric tensors existed. There is a fine distinction between the new metric tensor $\mathcal{M}_{1,p}^n$ and $\mathcal{M}_{1,p}^h$ proposed by Huang and Russell [26] that the former refers to $\text{tr}(\mathcal{H})$ and the latter involves $\|\mathcal{H}\|$. In some cases, the two metric tensors are pretty much alike. However, when dealing with the complex problems, e.g., with multiple layers, the effect of the former is superior to the latter for mesh generation. Numerical results show that the corresponding convergent rates are always almost optimal.

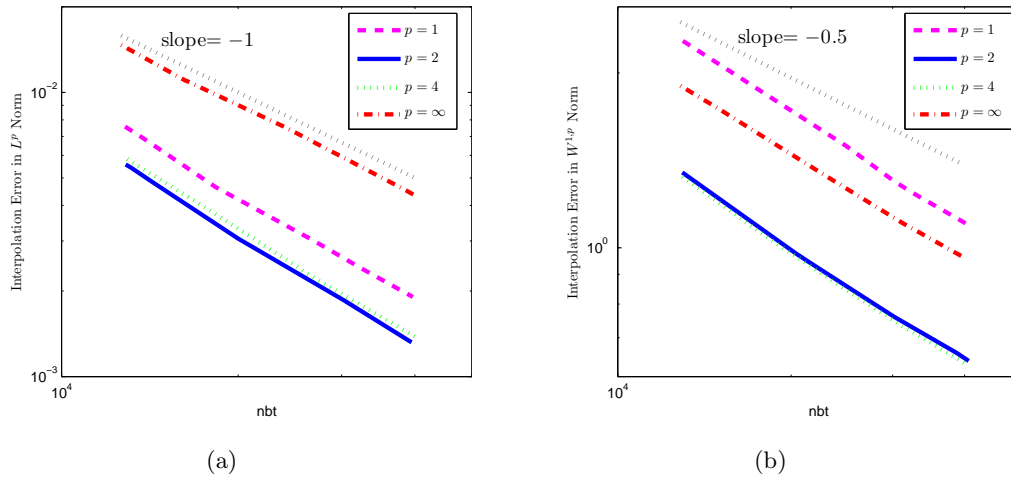


Figure 6: Example 3: Interpolation error and its gradient in L^p norm

References

- [1] A. Agouzal, K. Lipnikov, Y. Vassilevski, Adaptive generation of quasi-optimal tetrahedral meshes, East-West J. Numer. Math. 7 (1999) 223C244.
- [2] A. Agouzal, K. Lipnikov, Y. Vassilevski, Hessian-free metric-based mesh adaptation via geometry of interpolation error, Comp. Math. Math. Phys. 50 (1) (2010) 124-138.
- [3] A. Agouzal, Y. Vassilevski, Minimization of gradient errors of piecewise linear interpolation on simplicial meshes, Comput. Meth. Appl. Mech. Eng. 199 (2010) 2195-2203.
- [4] D. Ait-Ali-Yahia, W. Habashi, A. Tam, M.-G. Vallet, M. Fortin, A directionally adaptive methodology using an edge-based error estimate on quadrilateral grids, Int. J. Numer. Methods Fluids 23 (1996) 673-690.
- [5] T. Apel, G. Lube, Anisotropic mesh refinement in stabilized Galerkin methods, Numer. Math. 74(3) (1996) 261-282.
- [6] R. Becker, An adaptive finite element method for the incompressible Navier-stokes equations on time-dependent domains, Ph.D. thesis, Ruprecht-Karls-Universität Heidelberg, 1995.
- [7] H. Borouchaki, P.L. George, F. Hecht, P. Laug and E. Saltel, Delaunay mesh generation governed by metric specifications Part I. Algorithms, finite elem. anal. des. 25 (1997) 61-83.
- [8] H. Borouchaki, P.L. George, B. Mohammadi, Delaunay mesh generation governed by metric specifications Part II. Applications, finite elem. anal. des. 25 (1997) 85-109.

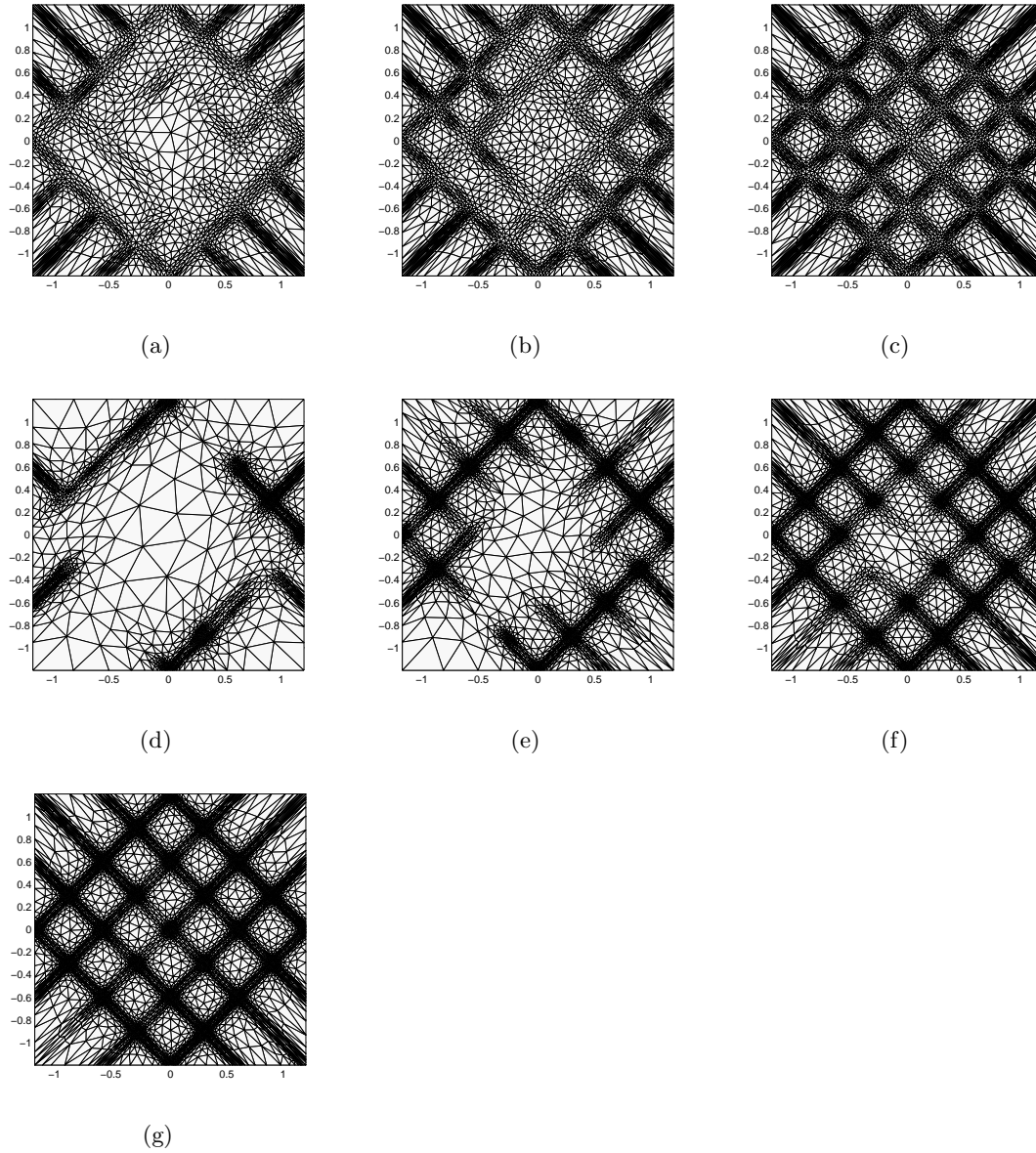


Figure 7: Example 3: Meshes generated by the metric tensors $\mathcal{M}_{1,2}$ after (a) 5 step, (b) 10 step, (c) 15 step, and $\mathcal{M}_{1,\infty}$ after (d) 5 step, (e) 10 step, (f) 15 step, (g) 20 step.

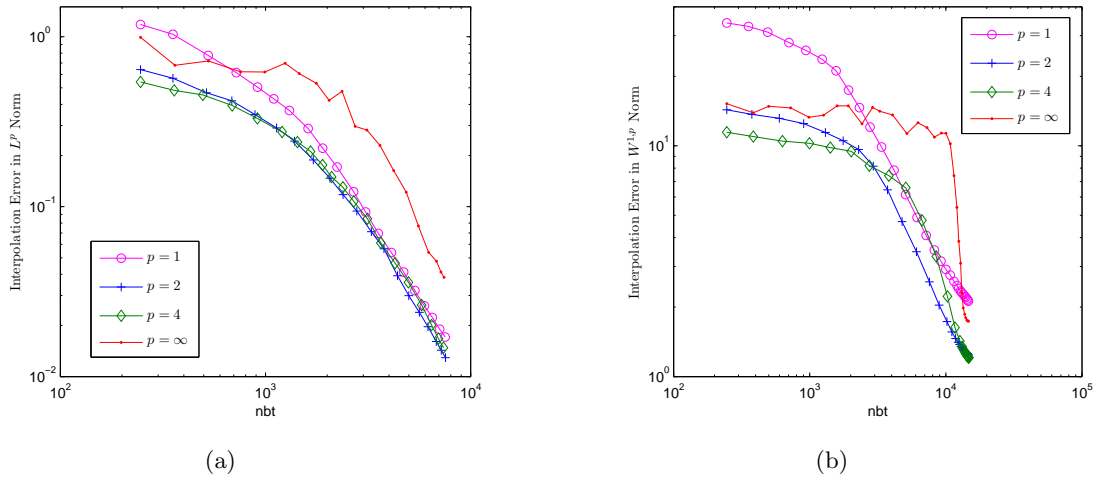


Figure 8: Example 3: Convergence history versus number of triangles by the metric tensor $\mathcal{M}_{0,p}$ and $\mathcal{M}_{1,p}$ for $p = 1, 2, 4, \infty$.

- [9] J.U. Brackbill, J.S. Saltzman, Adaptive zoning for singular problems in two dimensions, *J. Comput. Phys.* 46 (1982) 342-368.
- [10] G. Buscaglia, E. Dari, Anisotropic Mesh Optimization and its Application in Adaptivity, *Int. J. Numer. Meth. Eng.* 40(22) (1997) 4119-4136.
- [11] M.J. Castro-Díaz, F. Hecht, B. Mohammadi, O. Pironneau, Anisotropic unstructured mesh adaption for flow simulations, *Internat. J. Numer. Methods Fluids* 25(4) (1997) 475-491.
- [12] L. Chen, P. Sun, J. Xu, Optimal anisotropic meshes for minimizing interpolation errors in L^p -norm, *Math. Comp.* 76(257) (2007) 179-204.
- [13] E.F. D’Azevedo, R.B. Simpson, On optimal interpolation triangle incidences, *SIAM J. Sci. Statist. Comput.* 10 (1989) 1063-1075.
- [14] E.F. D’Azevedo, Optimal triangular mesh generation by coordinate transformation, *SIAM J. Sci. Stat. Comput.* 12 (1991) 755-786.
- [15] E.F. D’Azevedo, R.B. Simpson, On optimal triangular meshes for minimizing the gradient error, *Numer. Math.* 59 (1991) 321-348.
- [16] W. Dorfler, R. Nochetto, Small data oscillation implies the saturation assumption, *Numer. Math.* 91 (2002) 1-12.
- [17] A.S. Dvinsky, Adaptive grid generation from harmonic maps on Riemannian manifolds, *J. Comput. Phys.* 95 (1991) 450-476.

- [18] P. Frey, P.L. George, Mesh Generation: Application to Finite Elements, Hermes Science, Oxford and Paris, 2000.
- [19] R.V. Garimella, M.S. Shephard, Boundary layer meshing for viscous flows in complex domain. in: Proceedings of the 7th International Meshing Roundtable, Sandia National Laboratories, Albuquerque, NM, 1998, 107-118.
- [20] P.L. George, F. Hecht. Nonisotropic grids, in: J.F. Thompson, B.K. Soni, N.P. Weatherill, (Eds.), Handbook of Grid Generation, CRC Press, Boca Raton, 1999 20.1-20.29.
- [21] W.G. Habashi, J. Dompierre, Y. Bourgault, D. Ait-Ali-Yahia, M. Fortin, M.-G. Vallet, Anisotropic mesh adaptation: towards user-independent, mesh-independent and solver-independent CFD. Part I: general principles, Int. J. Numer. Meth. Fluids 32 (2000) 725-744.
- [22] W.G. Habashi, M. Fortin, J. Dompierre, M.-G. Vallet, Y. Bourgault, Anisotropic mesh adaptation: a step towards a mesh-independent and user-independent CFD, Barriers and challenges in computational fluid dynamics (Hampton, VA, 1996), 99-117, Kluwer Acad. Publ., Dordrecht, 1998.
- [23] F. Hecht, Bidimensional anisotropic mesh generator, Technical Report, INRIA, Rocquencourt, 1997.
- [24] W. Huang. Measuring mesh qualities and application to variational mesh adaptation. SIAM J. Sci. Comput. 26(5) (2005) 1643-1666.
- [25] W. Huang, Metric tensors for anisotropic mesh generation, J. Comput. Phys. 204(2) (2005) 633-665.
- [26] W. Huang and R.D. Russell, Adaptive Moving Mesh Methods, Series in Applied Mathematical Sciences, Springer, 2011.
- [27] O.P. Jacquotte, A mechanical model for a new grid generation method in computational fluid dynamics, Comput. Meth. Appl. Mech. Eng. 66 (1988) 323-338.
- [28] P. Knupp, L. Margolin, M. Shashkov, Reference jacobian optimization-based rezone strategies for arbitrary lagrangian eulerian methods, J. Comput. Phys. 176 (2002) 93-128.
- [29] R. Kornhuber, R. Roitzsch, On adaptive grid refinement in the presence of internal or boundary layers, IMPACT Comput. Sci. Eng. 2 (1990) 40-72.
- [30] J. Lang, An adaptive finite element method for convection-diffusion problems by interpolation techniques, Technical Report TR 91-4, Konrad-Zuse-Zentrum Berlin, 1991.

- [31] R. Li, T. Tang, and P. Zhang, Moving mesh methods in multiple dimensions based on harmonic maps, *J. Comput. Phys.* 170(2) (2001) 562-588.
- [32] E.J. Nadler, Piecewise linear approximation on triangulations of a planar region, Ph.D. Thesis, Division of Applied Mathematics, Brown University, Providence, RI, 1985.
- [33] H. Nguyen, M. Gunzburger, L. Ju, J. Burkardt, Adaptive anisotropic meshing for steady convection-dominated problems, *Comput. Meth. Appl. Mech. Eng.* 198 (2009) 2964-2981.
- [34] S. Owen, Meshing software survey, 1998, <http://www.andrew.cmu.edu/user/sowen/softsurv.html>.
- [35] J. Peraire, M. Vahdati, K. Morgan, O.C. Zienkiewicz, Adaptive remeshing for compressible flow computation, *J. Comp. Phys.* 72(2) (1987) 449-466.
- [36] W. Rachowicz, An anisotropic h-adaptive finite element method for compressible Navier-Stokes equations, *Comput. Meth. Appl. Mech. Eng.* 146 (1997) 231-252.
- [37] J. Remacle, X. Li, M.S. Shephard, and J.E. Flaherty, Anisotropic adaptive simulation of transient flows using discontinuous Galerkin methods, *Int. J. Numer. Meth. Eng.*, 62(7) (2005) 899-923.
- [38] S. Rippa, Long and thin triangles can be good for linear interpolation, *SIAM J. Numer. Anal.* 29 (1992) 257-270.
- [39] Y. Vassilevski, K. Lipnikov, Adaptive algorithm for generation of quasi-optimal meshes, *Comp. Math. Math. Phys.* 39 (1999) 1532C1551.
- [40] H. Xie, X. Yin, A strategy to derive metric tensors for anisotropic mesh generation, to appear.
- [41] S. Yamakawa and K. Shimada, High quality anisotropic tetrahedral mesh generation via ellipsoidal bubble packing. in: *Proceedings of the 9th International Meshing Roundtable*, Sandia National Laboratories, Albuquerque, NM, 2000. Sandia Report 2000-2207, 263-273.
- [42] X. Yin, H. Xie, A-posteriori error estimators suitable for moving mesh methods under anisotropic meshes, to appear.
- [43] O.C. Zienkiewicz, J. Wu, Automatic directional refinement in adaptive analysis of compressible flows, *Int. J. Numer. Meth. Eng.* 37 (1994) 2189-2210.